Mol Cell Biochem (2013) 384:59–69
DOI 10.1007/s11010-013-1781-9

Rotenone-induced oxidative stress and apoptosis in human liver HepG2 cells

M. A. Siddiqui · J. Ahmad · N. N. Farshori · Q. Saquib · S. Jahan · M. P. Kashyap · M. Ahamed · J. Musarrat · A. A. Al-Khedhairy

Received: 9 June 2013 / Accepted: 9 August 2013 / Published online: 21 August 2013

Abstract Rotenone, a commonly used pesticide, is well documented to induce selective degeneration in dopaminergic neurons and motor dysfunction. Such rotenone-induced neurodegenration has been primarily suggested through mitochondria-mediated apoptosis and reactive oxygen species (ROS) generation. But the status of rotenone induced changes in liver, the major metabolic site is poorly investigated. Thus, the present investigation was aimed to study the oxidative stress-induced cytotoxicity and apoptotic cell death in human liver cells-HepG2 receiving experimental exposure of rotenone (12.5–250 μM) for 24 h. Rotenone depicted a dose-dependent cytotoxic response in HepG2 cells. These cytotoxic responses were in concurrence with the markers associated with oxidative stress such as an increase in ROS generation and lipid peroxidation as well as a decrease in the glutathione, catalase, and superoxide dismutase levels. The decrease in mitochondrial membrane potential also confirms the impaired mitochondrial activity. The events of cytotoxicity and oxidative stress were found to be associated with up-regulation in the expressions (mRNA and protein) of pro-apoptotic markers viz., p53, Bax, and caspase-3, and down-regulation of anti-apoptotic marker Bcl-2. The data obtain in this study indicate that rotenone-induced cytotoxicity in HepG2 cells via ROS-induced oxidative stress and mitochondria-mediated apoptosis involving p53, Bax/Bcl-2, and caspase-3.

Keywords HepG2 cells · Rotenone · Cytotoxicity · Oxidative stress · Apoptosis

M. A. Siddiqui (✉) · J. Ahmad · Q. Saquib · J. Musarrat · A. A. Al-Khedhairy
Department of Zoology, College of Science, King Saud University, P.O. Box 2455, Riyadh 11451, Saudi Arabia
e-mail: maqsoodahmads@gmail.com; masiddiqui@ksu.edu.sa

N. N. Farshori
Department of Pharmacognosy, College of Pharmacy, King Saud University, Riyadh, Saudi Arabia

S. Jahan · M. P. Kashyap
In Vitro Toxicology Laboratory, CSIR-Indian Institute of Toxicology Research, Lucknow, India

M. Ahamed
King Abdullah Institute for Nanotechnology, King Saud University, Riyadh, Saudi Arabia

Introduction

Rotenone is a plant-derived pesticide, commonly used to protect crops from pests across the world since a long time [1]. It is a neurotoxicant that specifically inhibits the flow of electrons through the mitochondrial respiratory chain by binding with mitochondrial complex-I [2–4], and is known to cross blood brain barrier and gets accumulated in sub cellular organelles [5]. Rotenone is also well known to inhibit the biochemical processes at the cellular level, and can block electron transfer from complex to ubiquinone, resulting blocking of the oxidative phosphorylation, and an increase in reactive oxygen species (ROS) generation [1, 6]. A number of studies have evaluated the effects of rotenone under both in vitro [7] and in vivo conditions [1]. Studies have shown that rotenone is capable to induce apoptosis in various cells derived from human B cell lymphomas [8], promyelocytic leukemias [9], and neuroblastomas [10, 11]. Our group has also reported that rotenone induces oxidative stress-mediated cytotoxicity in rat pheochromocytoma cells-PC12 cell line [12], and in human breast adenocarcinoma-MCF-7 cell line [13]. Rotenone-induced mitochondrial complex-I inhibition results in generation of free radicals and thereby

induces the oxidative stress [14]. Experimental exposure of rotenone has been documented to cause detrimental effect under in vitro condition [15, 16], through environmental exposure [17], and in occupational setups [18]. These detrimental effects of rotenone are reported due to dysfunction of Complex-I of the mitochondrial electron transport chain, however, the mechanisms through which systemic Complex-I dysfunction produce toxicity are poorly understood. Hence, the present investigations were aimed to study the association between rotenone-induced cytotoxicity, ROS-induced oxidative stress, and mitochondria-mediated apoptosis in human liver cells-HepG2. Since, liver is a major metabolic site for xenobiotics and is known to be the primary target organ targeted by variety of chemicals/drugs. HepG2 cells were selected as test model due to their metabolic active nature and the expression of most of the marker gene proteins of human hepatocytes as in liver [19–21]. Besides this, HepG2 cells are also a well established model to study the xenobiotics-induced alterations in the expression and activity of cytochrome P450s (CYPs) [22–24]. HepG2 cell line is also among the most commonly used cell lines to evaluate the pesticides-induced toxicity and detoxification [25–27].

Materials and methods

Cell culture

HepG2 cells were grown in Dulbecco's modified eagle's medium (DMEM) supplemented with 10 % fetal bovine serum (FBS), 0.2 % sodium bicarbonate, and antibiotic/antimycotic solution (100×, 1 ml/100 ml of medium, Invitrogen, Life technologies, USA). The cells were maintained in 5 % CO_2–95 % atmosphere under high humidity at 37 °C. Cells were assessed for cell viability by trypan blue dye exclusion assay as described earlier by Pant et al. [28] and batches showing more than 98 % cell viability were used in the experiments.

Reagents and consumables

All the specified chemicals, reagents, and diagnostic kits were procured from Sigma Chemical Company Pvt. Ltd., St. Louis, MO, USA, unless otherwise stated. DMEM, antibiotics/antimycotics solution, and FBS were purchased from Sigma company, USA. Culture wares and other plastic consumables used in the study were procured from Nunc, Denmark.

Experimental design

HepG2 cells were exposed to various concentrations (12.5–250 μM) of rotenone for 24 h. Cells receiving rotenone were studied for cytotoxicity assays by MTT and NRU assays and morphological alterations. Furthermore, oxidative stress markers, i.e., lipid peroxidation (LPO), glutathione (GSH), catalase, superoxide dismutase (SOD), ROS, and mitochondrial membrane potential (MMP) were studied. Rotenone-induced apoptotic marker genes associated with mitochondria-mediated apoptosis by western blotting and RT-PCR^q were also studied.

MTT assay

Percent cell viability was assessed using the 3-(4,5-dimethylthiazol-2-yl)-2,5-diphenyl tetrazolium bromide (MTT) assay as described [29]. In brief, cells (1×10^4) were allowed to adhere for 24 h in CO_2 incubator at 37 °C in 96-well culture plates. After the exposure, MTT (5 mg/ml of stock in PBS) was added (10 μl/well in 100 μl of cell suspension), and plates were incubated for 4 h. The supernatant was discarded and 200 μl of DMSO were added to each well and mixed gently. The developed color was read at 550 nm. Untreated sets were also run under identical conditions and served as control.

Neutral red uptake (NRU) assay

NRU assay was carried out following the protocol described [30]. After the exposure, the medium was aspirated and cells were washed twice with PBS, and incubated for 3 h in a medium supplemented with neutral red (50 μg/ml). The medium was then washed off rapidly with a solution containing 0.5 % formaldehyde and 1 % calcium chloride. Cells were subjected to further incubation of 20 min at 37 °C in a mixture of acetic acid (1 %) and ethanol (50 %) to extract the dye. The plates were read at 540 nm. The values were compared with the control sets run under identical conditions.

Morphological analysis

Morphological changes in HepG2 cells exposed with rotenone were observed to determine the alterations induced by rotenone. All the cells were exposed to increasing concentrations (12.5–250 μM) of rotenone for 24 h and cell images were taken using an inverted phase contrast microscope at 20× magnification.

Lipid peroxidation (LPO)

LPO was performed using thiobarbituric acid (TBA)-reactive substances protocol [31]. In brief, after the exposure, HepG2 cells were collected by centrifugation and sonicated in ice cold potassium chloride (1.15 %) and centrifuged for 10 min at 3,000×g. Resulting supernatant (1 ml) was added to 2 ml of TBA reagent (15 % TCA,

0.7 % TBA and 0.25 N HCl) and heated at 100 °C for 15 min in a boiling bath. Then samples were placed in cold and centrifuged at 1,000×*g* for 10 min. Absorbance of the supernatant was measured at 535 nm.

Glutathione (GSH) content

Intracellular GSH content was estimated as described [32] with specific modifications. In brief, after respective exposure, cells were collected by centrifugation and cellular protein were precipitated by incubating 1 ml sonicated cell suspension with 1 ml TCA (10 %) and placed on ice for 1 h followed by a 10 min centrifugation at 3,000 rpm. The supernatant was added to 2 ml of 0.4 M Tris buffer (pH 8.9) containing 0.02 M EDTA followed by an addition of 0.01 M 5,5'-dithionitrobenzoic acid (DTNB) to a final volume of 3 ml. The tubes were incubated for 10 min at 37 °C in water bath with shaking. The absorbance of yellow color developed was read at 412 nm.

Catalase activity

The activity of catalase in cells was assayed following the protocol [33] using H_2O_2 as substrate. Reaction mixture in a final volume of 1 ml consisted of phosphate buffer (pH 7.0), 0.08 µmol of H_2O_2, and enzyme protein. The enzyme activity was measured following the disappearance of H_2O_2 at 570 nm.

Superoxide dismutase (SOD) activity

The assay of SOD activity was carried out using protocol described [34]. In brief, the reaction was initiated at room temperature by adding 0.052 M sodium pyrophosphate buffer (pH 8.3), 186 µM phenozine methosulphate, 300 µM nitroblue tetrazolium, 780 µM NADH, sonicated enzyme, and distilled water in a final volume of 3 ml. The reaction was stopped after 1.5 min at room temperature by adding 1.0 ml acetic acid and then 4.0 ml of *n*-butanol. The mixture was allowed to stand for 10 min, centrifuged, and butanol layer was separated. The color intensity of chromogen in butanol was measured at 560 nm against butanol. A mixture devoid of enzyme containing cell suspension served as control.

Reactive oxygen species (ROS) generation

ROS generation was assessed using 2,7-dichlorodihydrofluorescein diacetate (DCFH-DA; Sigma Aldrich, USA) dye as a fluorescence agent following the protocol earlier described by us [30]. Following the exposure of rotenone for 24 h, cells were washed with PBS and incubated for 30 min in DCFH-DA (20 µM) containing incomplete culture medium in dark at 37 °C. Then, the cells were analyzed for intracellular fluorescence using fluorescence microscope.

Mitochondrial membrane potential (MMP)

MMP was measured following the protocol of Zhang et al. [35]. In brief, control and treated cells were washed twice with PBS. Then, the cells were further exposed with 10 µg/ml of Rhodamine-123 fluorescent dye for 1 h at 37 °C in dark. Again cells were washed twice with PBS. Then, fluorescence intensity of Rhodamine-123 was measured using fluorescence microscope by grabbing the images at 20× magnification.

Transcriptional changes

Alterations in the mRNA expression of apoptosis marker genes (p53, Bax, Bcl-2, and caspase-3) were studied following the protocol [36]. In brief, cells (1×10^6) were allowed to grow in 6-well culture plates. Following the exposure of cells to rotenone for 24 h, total RNA was isolated from both experimental and control sets using RNeasy mini Kit (Qiagen) according to the manufacturer's instructions. Concentration of the extracted RNA were determined using Nanodrop 8000 spectrophotometer (Thermo-Scientific) and the integrity of RNA were visualized on 1 % agarose gel using gel documentation system (Universal Hood II, BioRad). The first-strand cDNA was synthesized from 1 µg of total RNA by Reverse Transcriptase using M-MLV (Promega) and oligo (dT) primers (Promega) according to the manufacturer's protocol. Quantitative real-time PCR (RT-PCR^q) was performed by LightCycler® 480 instrument (Roche Diagnostics, Rotcreuz, Switzerland). Two microliter of template cDNA was added to the final volume of 20 µl of reaction mixture. Real-time PCR cycle parameters included 10 min at 95 °C followed by 40 cycles involving denaturation at 95 °C for 15 s, annealing at 60 °C for 20 s, and elongation at 72 °C for 20 s. The sequences of the specific sets of primer for p53, Bax, Bcl-2, caspase-3, and β-actin used in this study are given in our previous publication [37]. Expressions of selected genes were normalized to β-actin gene, which was used as an internal housekeeping control. All the real-time PCR performed in triplicate and data was expressed as the mean of at least three independent experiments.

Protein expression (Western blotting)

Alterations in the expression of selected marker proteins (p53, Bax, Bcl-2, and caspase-3) associated with apoptosis were carried out by western immunoblotting as described earlier [30]. In brief, after respective exposure, cells were

washed twice with ice-cold PBS (pH 7.4) and centrifuged at 1,000 rpm for 10 min. Cell pellets were lysed using Cell Lysis Reagent (Catalog No# C2978, Sigma, USA) in the presence of 1× protein inhibitor cocktail (Catalog No# P8340, Sigma, USA). Equal amount (50 µg/well) of proteins was loaded in 10 % Tricine-SDS gel and electrophoresis was carried out. Following electrophoresis, protein bands from the gel were transferred on polyvinylidene fluoride membrane (Millipore, Bedford, MA, USA) in an electrophoresis transfer apparatus (BioRad, Hercules, CA, USA). The membrane was blocked overnight in TBST (30 mM Tris, pH 7.5, 150 mM NaCl and 0.1 % Tween 20) containing 5 % non-fatty milk. Membranes were then probed with primary antibodies specific for Bax (1:500, Santa Cruz, USA), Bcl-2, caspase-3 (1:1,000, CST, USA), and β-Actin (1:2,000, Santa Cruz, USA). After several washings with TBST, membrane was re-incubated with horseradish peroxidase-conjugated secondary antibody (goat anti-rabbit for Bax and cleaved-caspase-3, goat anti-mouse for all others) for 2 h at room temperature. Then, the blots were developed by using TMB–H_2O_2 (Sigma, USA). Picture of specific band were taken by Gel Documentation System (Alpha Innotech, USA) and densitometry was done by AlphaEaseTM FC StandAlone V. 4.0.0 software.

Protein estimation

Protein estimation of each sample was done following the method of Lowry et al. [38] using bovine serum albumin as a reference standard.

Statistical analysis

Results were expressed as mean ± standard error of three experiments. Statistical analysis was performed using one-way analysis of variance (ANOVA) and post hoc Dunnett's test was applied to compare values between control and treated groups. The values depicting $p < 0.05$ were considered as statistically significant.

Results

Cytotoxicity assessment

The cytotoxic effect of rotenone was evaluated by MTT and NRU assays. The percent cell viability observed by MTT and NRU assays are presented in Figs. 1 and 2. The results showed that rotenone significantly reduced the cell viability of HepG2 cells in a concentration-dependent manner (Fig. 1). The cell viability at 12.5, 25, 50, 100, and 250 µM concentrations of rotenone were recorded 95, 82, 70, 58, and 46 %, respectively by MTT assay (Fig. 1).

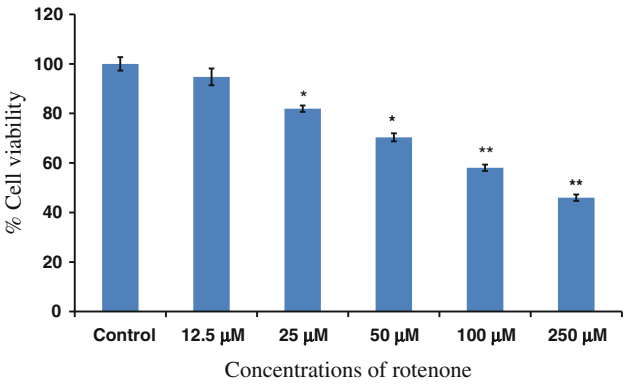

Fig. 1 Cytotoxicity assessment by MTT assay in HepG2 cells following the exposure of various concentrations of rotenone for 24 h. Values are mean ± SE of three independent experiments. (*$p < 0.01$, **$p < 0.001$ vs control)

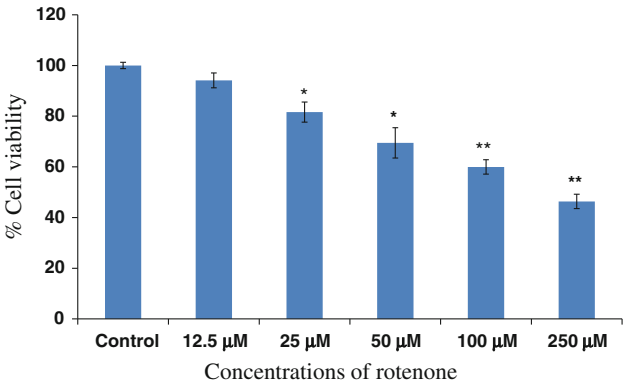

Fig. 2 Cytotoxicity assessment by neutral red uptake (NRU) assay in HepG2 cells following the exposure of various concentrations of rotenone for 24 h. Values are mean ± SE of three independent experiments. (*$p < 0.01$, **$p < 0.001$ vs control)

Similar kinds of results were also found in HepG2 cells exposed with various concentrations of rotenone by NRU assay (Fig. 2). The results showed that the rotenone significantly reduced the viability of HepG2 cells in a concentration-dependent manner (Fig. 2). The cell viability at 12.5, 25, 50, 100, and 250 µM concentrations of rotenone were found 94, 81, 69, 60, and 46 %, respectively (Fig. 2). Rotenone at 12.5 µM and lower concentrations did not cause any adverse effect on cell viability of HepG2 cells (Figs. 1, 2).

Morphological changes

The morphological changes observed in HepG2 cells after the exposure of rotenone for 24 h are shown in Fig. 3. Alterations in the morphology of HepG2 cells after the exposure of rotenone were observed under phase contrast inverted microscope. The cells indicated the most

prominent effects after the exposure of rotenone, and changes in their morphology were found in concentration-dependent manner. Cells exposed to 25 μM and above concentrations of rotenone reduced the normal morphology of the HepG2 cells and cell adhesion capacity in comparison to control (Fig. 3). Most of the cells at 250 μM of rotenone lost their typical morphology and appeared smaller in size, shrunken, and rounded (Fig. 3).

Glutathione level

Depletion in GSH level in cultured HepG2 cells exposed to 12.5–250 μM concentrations of rotenone for 24 h are summarized in Fig. 4a. The result indicates that rotenone decreased the GSH levels in a dose-dependent manner. Fig. 4a shows a significant decrease in the GSH activity at higher concentrations as compared to the untreated control. A concentration-dependent significant decrease of 20, 33, 44, and 55 % ($p < 0.001$) were observed in GSH activity at 25, 50, 100, and 250 μM of rotenone, respectively as compared to untreated control (Fig. 4a).

Lipid peroxidation

The rotenone-induced LPO in HepG2 cells are summarized in Fig. 4b. A concentration-dependent significant increase in LPO was also observed. An increase of 12, 32, 45, and 57 % at 25, 50, 100, and 250 μM, respectively were found in HepG2 cells exposed for 24 h (Fig. 4b).

Catalase activity

The results of catalase activity are summarized in Fig. 4c. A clear-cut significant decrease of 19, 34, 42, and 52 % were observed at 25, 50, 100, and 250 μM of rotenone, respectively as compared to untreated control (Fig. 4c).

Superoxide dismutase activity

SOD levels in HepG2 cells exposed to 12.5–250 μM of rotenone for 24 h are presented in Fig. 4d. A concentration-dependent decrease in the level of SOD was also observed in HepG2 cells. The decrease in SOD activity at 50 μM (12 %), 100 μM (25 %), 250 μM (37 %) were observed as compared to untreated control (Fig. 4d).

ROS generation

Statistically significant ($p < 0.001$) ROS generation was observed in HepG2 cells after the exposure of rotenone at 25, 50, and 100 μM concentrations for 24 h (Fig. 5A, B). The increase in ROS generation was concentration-dependent i.e., 23, 46, and 69 % of untreated control

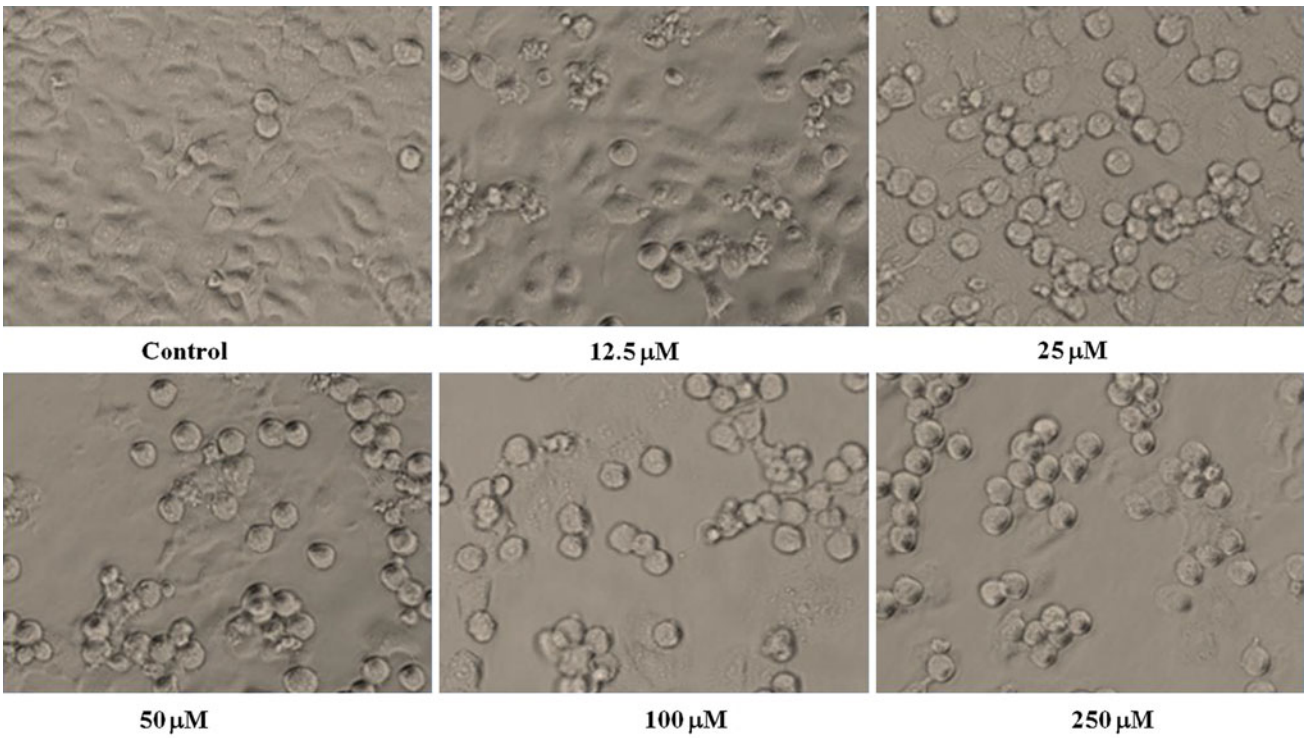

Fig. 3 Morphological changes in HepG2 cells exposed to various concentrations of rotenone for 24 h. Images were taken using an inverted phase contrast microscope at ×20 magnification

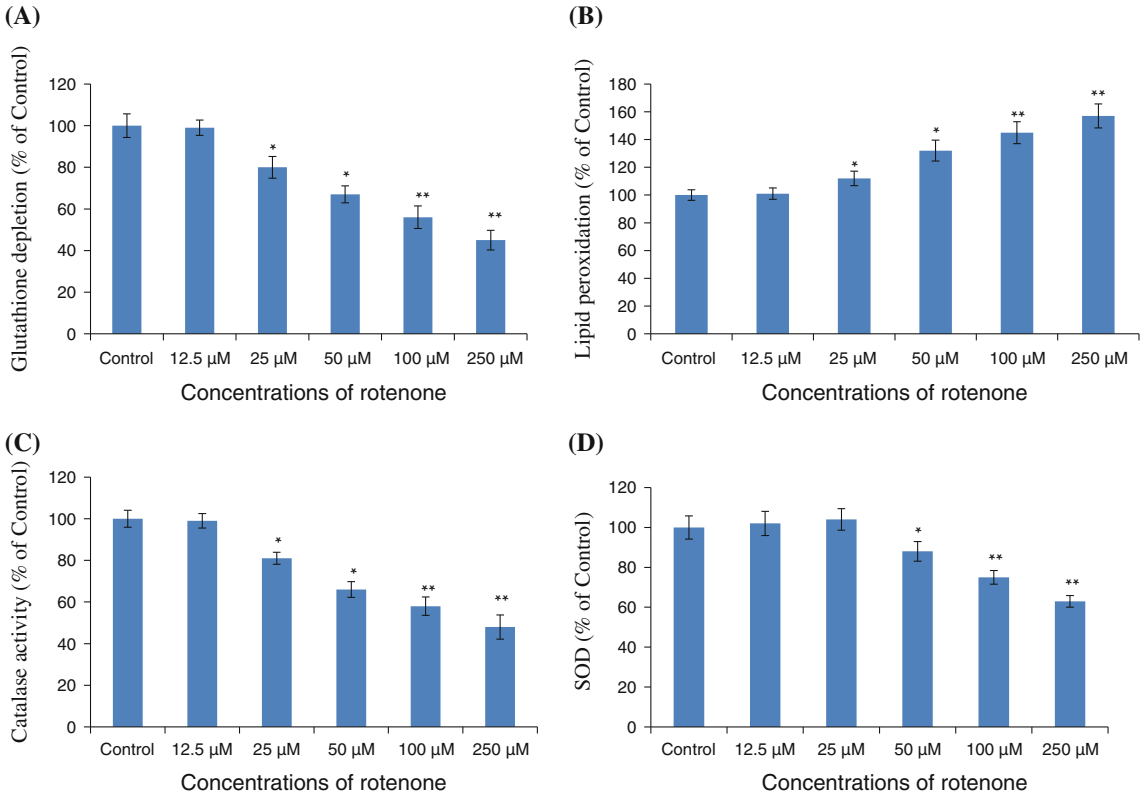

Fig. 4 Rotenone-induced oxidative stress in HepG2 cells exposed for 24 h. **a** Glutathione depletion; **b** Lipid peroxidation; **c** Catalase activity; **d** Superoxide dismutase (SOD). Values are mean ± SE of three independent experiments. (*$p < 0.01$, **$p < 0.001$ vs control)

following the exposure of 25, 50, and 100 μM of rotenone, respectively.

Mitochondrial membrane potential

The effect of rotenone exposure on MMP was evaluated in HepG2 cells. A concentration-dependent statistically significant ($p < 0.001$) decrease in the level of MMP was observed in HepG2 cells after the exposure of rotenone at 25, 50, and 100 μM concentrations for 24 h (Fig. 6A, B). Decrease in MMP was observed 14, 29, and 45 % at 25, 50, and 100 μM of rotenone, respectively as compared to untreated control (Fig. 6A, B).

Transcriptional changes in apoptosis markers

The alterations in the levels of mRNA expression of selected apoptosis marker genes in HepG2 cells exposed to rotenone for 24 h are presented in Fig. 7a–d. A significant ($p < 0.05$) upregulation in the expression of pro-apoptotic genes, i.e., p53 (2.15 fold), Bax (1.77 fold), Caspase-3 (1.34 fold), were observed at 100 μM concentration, whereas, anti-apoptotic gene Bcl-2 (0.45 fold) was significantly downregulated at 100 μM of rotenone.

Translational changes in apoptosis markers

Western blot analyses for apoptotic proteins were further used to study the level of protein expression in HepG2 cells exposed to rotenone for 24 h. The results of western blot analyses are shown in Fig. 8a–d. Cells exposed to rotenone at 100 μM showed a significant up-regulation in the expressions of p53 (2.1 fold), Bax (2.3 fold), and caspase-3 (twofold), whereas, the expression of Bcl-2 protein was down-regulated by 0.65 fold, respectively.

Discussion

In this study, MTT and NRU assays were used to determine the cytotoxicity of rotenone in human liver carcinoma (HepG2) cells. We found from the present investigations that these assays indicate a concentration-dependent decrease in the percent cell viability of HepG2 cells after the exposure of rotenone for 24 h. Results showed that rotenone exposure modulates the viability of HepG2 cells. The concentrations 25 μM and above showed a significant decrease ($p < 0.01$) in the percent cell viability of HepG2 cells compared to the untreated control. Findings from our

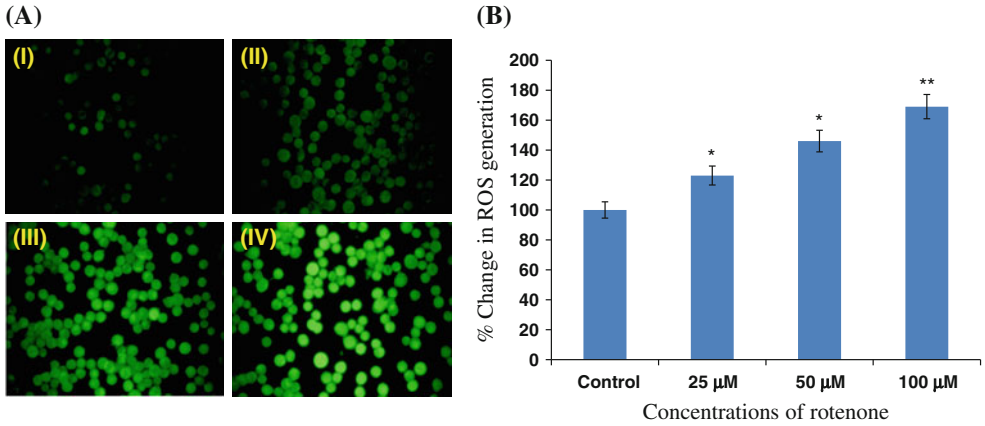

Fig. 5 **A** Rotenone-induced ROS generation in HepG2 cells. ROS generation was studied using dichlorofluorescindiacetate (DCFH-DA) dye after the exposure of rotenone for 24 h. (*a*) Control; (*b*) 25 µM; (*c*) 50 µM; and (*d*) 100 µM of rotenone. **B** Percent induction of ROS generation in HepG2 cells following the exposure of various concentrations of rotenone for 24 h. (*$p < 0.01$, **$p < 0.001$ vs control)

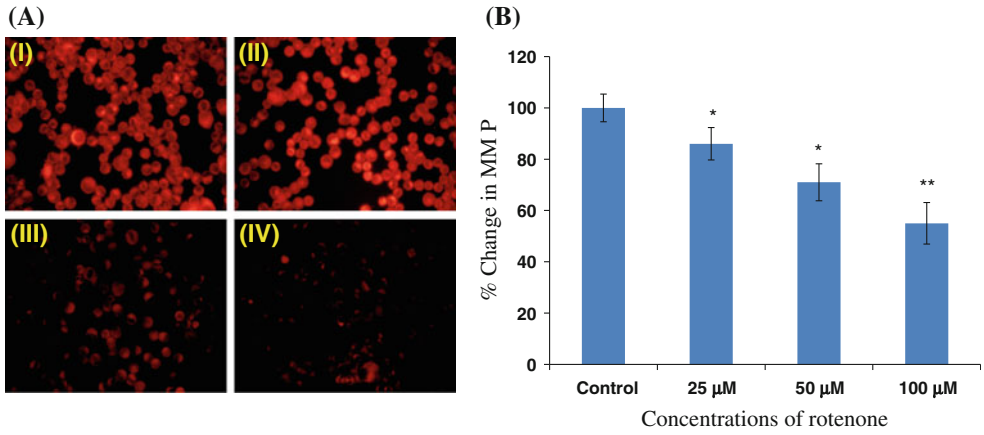

Fig. 6 **A** Rotenone-induced reduction in the intensity of mitochondrial membrane potential (MMP) in HepG2 cells exposed for 24 h. MMP was studied using Rh123 fluorescent dye. (*a*) Control; (*b*) 25 µM; (*c*) 50 µM; and (*d*) 100 µM of rotenone. **B** Percent induction of MMP in HepG2 cells following the exposure of various concentrations of rotenone for 24 h. (*$p < 0.01$, **$p < 0.001$ vs control)

study are well consistent with the previous studies that reports the toxicity of rotenone in various cell types [27, 39, 40], and by the other pesticides in HepG2 cells [25, 26, 41]. In our previous studies, we have also reported that higher concentrations of rotenone-induced cytotoxicity in PC12 and MCF-7 cells by MTT and NRU assays [12, 13]. Oxidative stress can be viewed as an imbalance between pro-oxidants and antioxidants, both excess production of ROS and LPO, and deficiency in cellular antioxidant defenses e.g., GSH, catalase, and SOD levels. Moreover, rotenone is a known inhibitor of mitochondrial complex-I, and the mitochondria are the major subcellular organelles responsible for ROS production [40, 42]. The role of rotenone in triggering ROS generation in HepG2 cells indicates that the higher concentrations of rotenone resulted in enhanced ROS generation, which led to oxidative stress. Our results showed that rotenone depleted intracellular GSH, catalase, and SOD levels, and increased the level of LPO. Results indicating that these alterations in HepG2 cells may be due to the oxidative stress, which is a mediator of rotenone cytotoxicity. It is well known that the GSH, catalase, SOD, and LPO are crucial components of cellular antioxidant defenses and play a major role in protecting cells against oxidative stress and cellular injuries [43–45]. Another oxidative stress marker ROS production was also examined. ROS are continuously generated through normal cellular metabolisms or by exogenous insults. In this study, rotenone induced intracellular ROS production in a concentration-dependent manner. Similar to other oxidative stress markers, ROS production was also significantly observed in HepG2 cells, since the excess generation of ROS has been considered as a crucial mediator of cell death [46–48]. We also found that rotenone decreases the MMP in HepG2 cells. As shown in Fig. 6A, B, HepG2 cells exposed to rotenone reduced MMP in a dose-dependent manner are well agreement with Dornetshuber et al. [49], suggesting a less preserved mitochondrial integrity. It might be the oxygen radicals

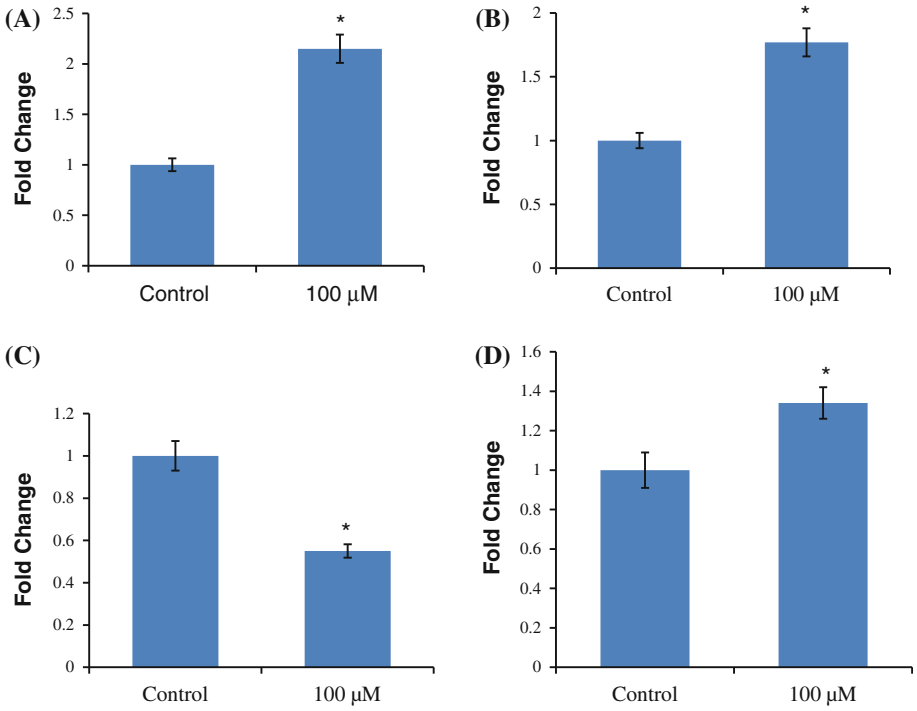

Fig. 7 Real Time-PCR analysis of alterations in the mRNA expression of various apoptosis genes. **a** p53; **b** Bax; **c** Bcl-2; **d** Caspase-3 in HepG2 cells exposed for 24 h. The data provided are mean + SE from three separate experiments. *$p < 0.05$ versus control

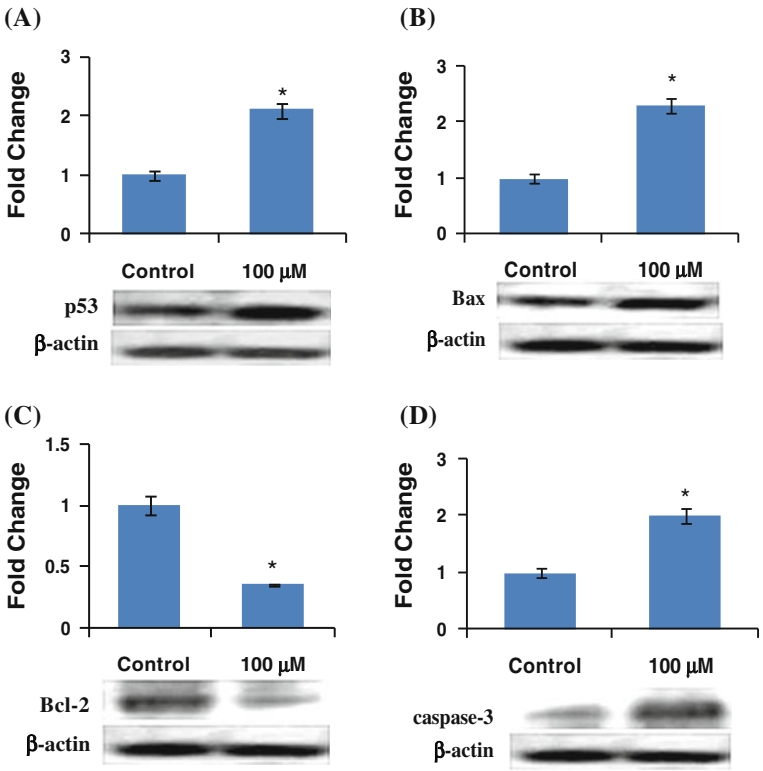

Fig. 8 Rotenone-induced alterations in the protein expression of apoptosis markers. **a** p53; **b** Bax; **c** Bcl-2; **d** Caspase 3 in HepG2 cells exposed for 24 h. Data are expressed as mean + SE. *$p < 0.05$ versus control

produced during mitochondrial respiration which suggests a possible correlation between oxidative stress and mitochondrial activity [50], which leads to apoptosis [51].

The involvement of mitochondrial chain complexes in ROS-induced apoptotic changes has been reported [52]. These apoptotic changes are known to follow different pathways [53, 54]. Mitochondria-dependent apoptotic pathway is also known to be involved in cell death [30, 36]. In this study, we observed that rotenone significantly up-regulates the expression (mRNA and protein) of p53, Bax,

caspase-3, and down-regulated Bcl-2 in a concentration-dependent manner. In general, transcriptional changes were well coordinated with translational changes in HepG2 cells exposed to rotenone for 24 h. In the present study, after the exposure of various concentrations of rotenone, the expression of Bax, caspase-3, and p53 was found to be increased significantly, while Bcl-2 expression decreased in a concentration-dependent manner. The present study, confirmed that rotenone may induce apoptosis in HepG2 cells. Our data reveals that rotenone-induced caspase-3 activity and the apoptotic response of rotenone are associated with decreased Bcl-2 expression and increased Bax expression. This suggests that HepG2 cells are able to undergo apoptosis when stimulated by rotenone. Alterations in the p53 gene are the most frequent genetic change in human cancers. It is estimated that about 50 % of all human malignancies contain mutations of this gene [55, 56]. However, a higher level of cytoplasmic p53 protein interacts with mitochondria, thereby promoting mitochondrial membrane permeabilization [57], and plays an important role in the regulation of apoptosis [58]. As p53 has been reported to play a role of transcriptional activator, active p53 induces the transcription of many genes, including many apoptosis-related genes. The Bax gene has recently been found to be a transcriptional target of p53 and could be up-regulated in response to a variety of p53-dependent apoptosis triggers [56, 59]. Thus, the alterations in the expression profile of marker genes in this study indicate that p53 triggers the mitochondrial apoptotic cascade in HepG2 cells exposed to rotenone. Our results demonstrate that up-regulated levels of p53 promote induction in the expression of pro-apoptotic Bax, whereas down-regulation in the expression of anti-apoptotic Bcl-2 protein. Therefore, this imbalance in the ratio of Bax/Bcl-2 could lead the dissipation in MMP. Finally, dysfunctional mitochondria could release cytochrome-c in cytosol, which could activate caspase-3 via the activation of procaspase-9. In the case of rotenone-induced apoptosis, imbalance of Bax/Bcl-2 protein may be an upstream event followed by mitochondrial-mediated activation of caspase-3, a final executer caspase, which leads to cell apoptosis. Our result demonstrates that the up-regulation of Bax is due to the activated p53 and hence, it is in agreement with the observation on the collapse of MMP in mitochondria because Bax and Bax-like proteins have been reported to initiate caspase-independent death via channel forming activity, which promotes the mitochondrial permeability, increased ability to bind DNA and mediate transcriptional activation [60, 61].

In conclusion, the present study demonstrated that rotenone-induced cytotoxicity and oxidative stress in a concentration-dependent manner in human liver cells (HepG2). The apoptosis was found to be associated with ROS and oxidative stress. Both the mRNA and protein expressions of p53 and apoptotic genes (Bax and caspase-3) were up-regulated while the anti-apoptotic gene Bcl-2 was down-regulated. These findings suggest that oxidative stress plays an important role in rotenone-induced cytotoxicity and apoptosis in human liver cells.

Acknowledgments Financial support from National Plan for Sciences and Technology (NPST Project No. 10-ENV1314-02) and DNA Research Chair, King Saud University, Riyadh is acknowledged.

References

1. Radad K, Rausch WD, Gille G (2006) Rotenone induces cell death in primary dopaminergic culture by increasing ROS production and inhibiting mitochondrial respiration. Neurochem Int 49:379–386
2. Kitamura Y, Inden M, Miyamura A, Kakimura J, Taniguchi T, Shimohama S (2002) Possible involvement of both mitochondria and endoplasmic reticulum-dependent caspase pathways in rotenone-induced apoptosis in human neuroblastoma SH-SY5Y cells. Neurosci Lett 333:25–28
3. Sherer TB, Betarbet R, Testa CM, Seo BB, Richardson JR, Kim JH, Miller GW, Yagi T, Matsuno-Yagi A, Greenamyre JT (2003) Mechanism of toxicity in rotenone models of Parkinson's disease. J Neurosci 23:10756–10764
4. Cicchetti F, Drouin-Ouellet J, Gross RE (2009) Environmental toxins and Parkinson's disease: what have we learned from pesticide-induced animal models? Trends Pharmacol Sci 30:475–483
5. Lee J, Huang MS, Yang IC, Lai TC, Wang JL, Pang VF, Hsiao M, Kuo MY (2008) Essential roles of caspases and their upstream regulators in rotenone-induced apoptosis. Biochem Biophys Res Commun 371:33–38
6. Deng YT, Huang HC, Lin JK (2010) Rotenone induces apoptosis in MCF-7 human breast cancer cell-mediated ROS through JNK and p38 signaling. Mol Carcinog 49:141–151
7. Wang G, Qi C, Fan GH, Zhou HY, Chen SD (2005) PACAP protects neuronal differentiated PC12 cells against the neurotoxicity induced by a mitochondrial complex I inhibitor, rotenone. FEBS Lett 579:4005–4011
8. Armstrong JS, Hornung B, Lecane P, Jones DP, Knox SJ (2001) Rotenone-induced G2/M cell cycle arrest and apoptosis in a human B lymphoma cell line PW. Biochem Biophys Res Commun 289:973–978
9. Tada-Oikawa S, Hiraku Y, Kawanishi M, Kawanishi S (2003) Mechanism for generation of hydrogen peroxide and change of mitochondrial membrane potential during rotenone-induced apoptosis. Life Sci 73:3277–3288
10. Chung WG, Miranda CL, Maier CS (2007) Epigallocatechin gallate (EGCG) potentiates the cytotoxicity of rotenone in neuroblastoma SH-SY5Y cells. Brain Res 1176:133–142
11. Watabe M, Nakaki T (2004) Rotenone induces apoptosis via activation of bad in human dopaminergic SH-SY5Y cells. J Pharmacol Exp Ther 311:948–953
12. Siddiqui MA, Kashyap MP, Khanna VK, Yadav S, Al-Khedhairy AA, Musarrat J, Pant AB (2010) Association of dopamine DA-D2 receptor in rotenone-induced cytotoxicity in PC12 cells. Toxicol Ind Health 26:533–542
13. Siddiqui MA, Saquib Q, Ahamed M, Ahmad J, Al-Khedhairy AA, Abou-Tarboush FM, Musarrat J (2011) Effect of *Trans*-resveratrol on rotenone induced cytotoxicity in human breast adenocarcinoma cells. Toxicol Int 18:105–110

14. Swarnkar S, Singh S, Mathur R, Patro IK, Nath C (200) A study to correlate rotenone induced biochemical changes and cerebral damage in brain areas with neuromuscular coordination in rats. Toxicology 272:17–22
15. Olanow CW (2007) The pathogenesis of cell death in Parkinson's disease. Move Disord 22:S335–S342
16. Sai Y, Wu Q, Le W, Ye F, Li Y, Dong Z (2008) Rotenone-induced PC12 cell toxicity is caused by oxidative stress resulting from altered dopamine metabolism. Toxicol In Vitro 22: 1461–1468
17. Drechsel DA, Patel M (2008) Role of reactive oxygen species in the neurotoxicity of environmental agents implicated in Parkinson's disease. Free Radic Biol Med 44:1873–1886
18. Dhillon AS, Tarbutton GL, Levin JL, Plotkin GM, Lowry LK, Nalbone JT, Shepherd S (2008) Pesticide/environmental exposures and Parkinson's disease in East Texas. J Agromedicine 13:37–48
19. Zhang X, Yao Y, Lou Y, Jiang H, Wang X, Chai X, Zeng S (2010) Metabolism of ebracteolata compound B studied in vitro with human liver microsomes, HepG2 cells and recombinant human enzymes. Drug Metab Dispos 38:2157–2165
20. Birringer M, Lington D, Vertuani S, Manfredini S, Scharlau D, Glei M, Ristow M (2010) Proapoptotic effects of long-chain vitamin E metabolites in HepG2 cells are mediated by oxidative stress. Free Radic Biol Med 49:1315–1322
21. Kim JH, Kim D, Kim J, Hwang JK (2011) Euchresta horsfieldii Benn. Activates peroxisome proliferator-activated receptor α and regulates expression of genes involved in fatty acid metabolism in human HepG2 cells. J Ethnopharmacol 33:244–247
22. Dong H, Lin W, Wu J, Chen T (2010) Flavonoids activate pregnane × receptor-mediated *CYP3A4* gene expression by inhibiting cyclin-dependent kinases in HepG2 liver carcinoma cells. BMC Biochem 11:23
23. Yokota SI, Higashi E, Fukami T, Yokoi T, Nakajima M (2011) Human CYP2A6 is regulated by nuclear factor-erythroid 2 related factor 2. Biochem Pharmacol 81:289–294
24. Zhang Y, Zolfaghari R, Ross AC (2010) Multiple retinoic acid response elements cooperate to enhance the inducibility of CYP26A1 gene expression in liver. Gene 464:32–43
25. Moore PD, Yedjou CG, Tchounwou PB (2010) Malathion-induced oxidative stress, cytotoxicity and genotoxicity in human liver carcinoma (HepG2) cells. Environ Toxicol 25:221–226
26. Song MO, Lee CH, Yang HO, Freedman JH (2012) Endosulfan upregulates AP-1 binding and ARE-mediated transcription via ERK1/2 and p38 activation in HepG2 cells. Toxicology 292: 23–32
27. Zhang X, Zhou X, Chen R, Zhang H (2012) Radiosensitization by inhibiting complex I activity in human hepatoma HepG2 cells to X-ray radiation. J Radiat Res 53:257–263
28. Pant AB, Agarwal AK, Sharma VP, Seth PK (2001) In vitro cytotoxicity evaluation of plastic biomedical devices. Hum Exp Toxicol 20:412–417
29. Siddiqui MA, Singh G, Kashyap MP, Khanna VK, Yadav S, Chandra D, Pant AB (2008) Influence of cytotoxic doses of 4-hydroxynonenal on selected neurotransmitter receptors in PC-12 cells. Toxicol In Vitro 22:1681–1688
30. Siddiqui MA, Kashyap MP, Kumar V, Al-Khedhairy AA, Musarrat J, Pant AB (2010) Protective potential of trans-resveratrol against 4-hydroxynonenal induced damage in PC12 cells. Toxicol In Vitro 24:1592–1598
31. Buege JA, Aust SD (1978) Microsomal lipid peroxidation. Methods Enzymol 52:302–310
32. Chandra D, Ramana KV, Wang L, Christensen BN, Bhatnagar A, Srivastava SK (2002) Inhibition of fiber cell globulization and hyperglycemia-induced lens opacification by aminopeptidase inhibitor bestatin. Invest Ophthalmol Vis Sci 43:2285–2292
33. Sinha AK (1972) Colorimetric assay of catalase. Anal Biochem 47:389–394
34. Kakkar PS, Das B, Viswanathan PN (1984) A modified spectrophotometric assay of superoxide dismutase. Ind J Biochem Biophys 21:130–132
35. Zhang Y, Jiang L, Jiang L, Geng C, Li L, Shao J, Zhong L (2011) Possible involvement of oxidative stress in potassium bromate-induced genotoxicity in human HepG2 cells. Chem Biol Interact 189:186–191
36. Siddiqui MA, Kumar V, Kashyap MP, Agarwal M, Singh AK, Jahan S, Khanna VK, Al-Khedhairy AA, Musarrat J, Pant AB (2012) Short term exposure of 4-hydroxynonenal induces mitochondria mediated apoptosis in PC12 cells. Hum Exp Toxicol 31:336–345
37. Ahamed M, Akhtar MJ, Siddiqui MA, Ahmad J, Musarrat J, Al-Khedhairy AA, AlSalhi MS, Alrokayan SA (2011) Oxidative stress mediated apoptosis induced by nickel ferrite nanoparticles in cultured A549 cells. Toxicology 283:101–108
38. Lowry OH, Rosebrough NJ, Farr AL, Randall RJ (1951) Protein measurement with the Folin phenol reagent. J Biol Chem 193:265–275
39. Hongo H, Kihara T, Kume T, Izumi Y, Niidome T, Sugimoto H, Akaik A (2012) Glycogen synthase kinase-3b activation mediates rotenone-induced cytotoxicity with the involvement of microtubule destabilization. Biochem Biophys Res Commun 426:94–99
40. Swarnkar S, Singh S, Goswami P, Mathur R, Patro IK, Nath C (2012) Astrocyte activation: a key step in rotenone induced cytotoxicity and DNA damage. Neurochem Res 37:2178–2189
41. Juan-García A, Manyes L, Ruiz MJ, Font G (2013) Involvement of enniatin-induced cytotoxicity in human HepG2 cells. Toxicol Lett 218:166–173
42. Zhang HM, Zhang Y, Zhang BX (2011) The role of mitochondrial complex III in melatonin-induced ROS production in cultured mesangial cells. J Pineal Res 50:78–82
43. Armstrong JS, Jones DP (2002) Glutathione depletion enforces the mitochondrial permeability transition and causes cell death in Bcl-2 overexpressing HL 60 cells. FASEB J 16:1263–1265
44. Stanislawski L, Lefeuvre M, Bourd K, Soheili-Majd E, Goldberg M, P′erianin A (2003) TEGDMA-induced toxicity in human fibroblasts is associated with early and drastic glutathione depletion with subsequent production of oxygen reactive species. J Biomed Mater Res A 66:476–482
45. Herrera B, Murillo MM, A′lvarez-Barrientos A, Beltra′n J, Fern′andez M, Fabregat I (2004) Source of early reactive oxygen species in the apoptosis induced by transforming growth factor-beta in fetal rat hepatocytes. Free Radic Biol Med 36:16–26
46. Bergamini CM, Gambetti S, Dondi A, Cervellati C (2004) Oxygen, reactive oxygen species and tissue damage. Curr Pharm Des 10:1611–1626
47. Martindale JL, Holbrook NJ (2002) Cellular response to oxidative stress: signaling for suicide and survival. J Cell Physiol 192:1–15
48. Czaja MJ, Liu H, Wang Y (2003) Oxidant-induced hepatocyte injury from menadione is regulated by ERK and AP-1 signaling. Hepatology 37:1405–1413
49. Dornetshuber R, Heffeter P, Kamyar MR, Peterbauer T, Berger W, Lemmens-Gruber R (2007) Enniatin exerts p53-dependent cytostatic and p53-independent cytotoxic activities against human cancer cells. Chem Res Toxicol 20:465–473
50. Mronga T, Stahnke T, Goldbaum O, Richter-Landsberg C (2004) Mitochondrial 576 pathway is involved in hydrogen-peroxide induced apoptotic cell death of oligo- 577 dendrocytes. Glia 46:446–455
51. Sharma V, Anderson D, Dhawan A (2012) Zinc oxide nanoparticles induce oxidative DNA damage and ROS-triggered mitochondria mediated apoptosis in human liver cells (HepG2). Apoptosis 17:852–870

52. Galluzzi L, Morselli E, Kepp O, Tajeddine N, Kroemer G (2008) Targeting p53 to mitochondria for cancer therapy. Cell Cycle 7:1949–1955
53. Segui B, Legembre P (2010) Redistribution of CD95 into the lipid rafts to treat cancer cells? Recent Pat Anticancer Drug Discov 5:22–28
54. Kroemer G, Galluzzi L, Brenner C (2007) Mitochondrial membrane permeabilization in cell death. Physiol Rev 87:99–163
55. Bellamy CO, Prost S, Wyllie AH, Harrison DJ (1997) UV but not gammairradiation induces specific transcriptional activity of p53 in primary hepatocytes. J Pathol 183:177–181
56. Li J, Cheung H-Y, Zhang Z, Chan GKL, Fong W-F (2007) Andrographolide induces cell cycle arrest at G2/M phase and cell death in HepG2 cells via alteration of reactive oxygen species. Eur J Pharmacol 568:31–44
57. Moll UM, Wolff S, Speidel D, Deppert W (2005) Transcription independent pro-apoptotic functions of p53. Curr Opin Cell Biol 17:631–636
58. Yu J, Zhang L (2005) The transcriptional targets of p53 in apoptosis control. Biochem Biophys Res Commun 331:851–858
59. McGill G, Fisher DE (1997) Apoptosis in tumorigenesis and cancer therapy. Front Biosci 2:353–379
60. Lakin ND, Jackson SP (1999) Regulation of p53 in response to DNA damage. Oncogene 18:7644–7655
61. Xu J, Ji L-D, Xu L-H (2006) Lead-induced apoptosis in PC 12 cells: Involvement of p53, Bcl-2 family and caspase-3. Toxicol Lett 166:160–167